To be in the proceedings of
17th International Conference on Pattern Recognition
Cambridge, United Kindom, 23-26 AUG 2004

Automated Detection of Solar Loops by the Oriented Connectivity Method

Jong Kwan Lee Timothy S. Newman G. Allen Gary*
Dept. of Comp. Science, Univ. of Alabama in Huntsville *Marshall Space Flight Center/NASA
{jlee,tnewman}@cs.uah.edu Allen.Gary@nasa.org

Abstract

An automated technique to segment solar coronal loops from intensity images of the Sun's corona is introduced. It exploits physical characteristics of the solar magnetic field to enable robust extraction from noisy images. The technique is a constructive curve detection approach, constrained by collections of estimates of the magnetic field's orientation. Its effectiveness is evaluated through experiments on synthetic and real coronal images.

1. Introduction

The Sun is a dynamic force that greatly impacts the solar system. In particular, solar activity can impact terrestrial communication and weather. Solar physicists are currently attempting to gain a stronger understanding of solar dynamism, partially via study of solar magnetism.

Observing and analyzing the solar magnetic field from solar satellite images is one key means to study solar dynamism. In particular, solar physicists are interested in examining solar corona images. NASA's ongoing TRACE satellite mission, which collects high-resolution (512×512) intensity images of the Sun's corona several times per hour, is a preferred source of such images. (A sample TRACE image is shown in Fig. 1(a).) The primary examination task is to detect and identify the solar coronal loop structures in these images. Previously, automatic means to detect and identify such structures haven't been successful; current scientific study of solar coronal loops requires manual extraction of the loop structures from images. Detection of coronal loops is challenging, even using TRACE images, because the loop structures tend to have blurry boundaries and overlap in the imagery. Many loops also have low contrast sub-segments. (The intensity of such sub-segments is relatively lower than that of others.) In addition, there is impulse noise in the images.

In this paper, a new technique, the Oriented Connectivity Method, for automated segmentation of coronal loops from images of the Sun's corona is introduced. The technique exploits constraints based on physical properties to guide the curve detection process.

2. Related Work

A number of methods for representing, following, and linking edge structures in intensity images have been presented. For example, since the early 60's, starting with Freeman's [2] well-known chain coding, structure boundary representation mechanisms have been presented. Edge linkage approaches have also been described. For example, Makhervaks *et al.* [7] have recently presented an edge linkage process that joins edge structures using an edge-explorer operator that acts on a gradient vector field.

Curve feature detection methods have also been described. For instance, Canning *et al.* [1] have detected thin curve features by examining pixel neighborhoods to identify local gray level patterns that are consistent with the presence of an edge. Adjacent, compatible edge pixels are then linked. Jang and Hong [4] have detected curvilinear structures using skeleton extraction. They use Canny edge detection to define the boundary points of the regions in which the skeleton extraction will be performed.

Hough-based techniques [3] have also been used in curve detection. Their large parameter space for large images and for complex shapes, such as in our problem domain, is a difficulty, however. Active contour models (i.e., snakes [5]), which are typically defined as energy-minimizing splines, have also been widely used. A difficulty with using snakes for coronal loop detection is that there are many nearby loops and the loops cross each other, so it is easy for a single snake to lock onto components of multiple loops. Coronal loop crossings also complicate use of many other curve detection schemes.

Strous [10] has described a pixel labeling algorithm for coronal images. The algorithm labels a pixel as a member of a loop structure if the pixel's intensity is higher than those of more than two of the four cross-pairs in its 3×3 neighborhood (and as a non-member otherwise). Since the pixels on the central axis of the coronal loop structures are usually brighter than the neighboring pixels, Strous's algorithm detects most of the coronal loop *pixels*. It does not detect *loops* per se, however, as it has no process to link

pixels into loop structures. In addition, the algorithm falsely labels as loop pixels many noisy background pixels and many bright pixels not actually on coronal loops.

3. Coronal Loop Detection Methodology

Next, we describe our new Oriented Connectivity Method (OCM), which is based partly on Strous's loop pixel labeling [10]. The OCM constructively segments the coronal loops while simultaneously eliminating false loop pixels. The approach's processing includes steps that achieve joining of disconnected loop sub-segments, thus forming descriptions of complete loops. The Oriented Connectivity performs its loop segmentation by exploiting a physical constraint, namely the local orientation of the solar magnetic field. Since coronal loops align with the solar magnetic field, we exploit knowledge of the field to aid the linkage process.

Magnetic fields, including local fields in regions about the Sun, can be reasonably approximated in 3D space by a dipole field model [6]. One complexity in using a 3D spatial model to guide loop detection in the coronal intensity images is that such images record the projection of 3D structures onto 2D image space. The Sun's field is also a collection of many dipoles, and each one's position needs to be estimated. Thus, many points in 3D space, each with a different local magnetic field orientation, could project to each pixel. Some 3D-to-2D-projected loops could also cross.

Our approach exploits the dipole field model by, at each pixel labeled as a loop pixel after application of Strous's algorithm, considering a set of estimates of the 3D-to-2D-projected magnetic fields' orientations. We use these estimates to progressively link pixels with consistent magnetic field orientation. The set of estimates are taken from a set of azimuth maps (of the magnetic field) from a solar magnetogram. The positions of dipoles for the dipolar magnetic field model can be determined using the local minima and maxima of the magnetogram and a numerical method (e.g., Powell's minimization [9]). Each azimuth map records an estimate of the angular direction of the magnetic field and is defined for one height above the solar surface, so for small regions of the solar surface each azimuth map is a map of the magnetic field's orientations at a given height (i.e., in z). The azimuth can be derived from the vector sum of the x and y components (i.e., B_x and B_y) of the magnetic dipole flux density equation [8]:

$$B_x = 3B_o xz / r^5, \quad B_y = 3B_o yz / r^5, \qquad (1)$$

where x, y, and z are the Cartesian components of the magnetic field position vector, r is the magnitude of the position vector, and B_o is the magnetic force constant.

3.1. Preprocessing

The Strous's algorithm [10] (that our approach is based upon) produces a poor labeling when applied to a raw TRACE image, partially due to the known imaging effects described earlier. Thus, to remove impulse noise and to improve the contrast between the loops and the background, prior to applying the Strous algorithm, we have applied median filtering followed by unsharp masking as preprocessing steps. We empirically determined that 7×7 median filtering could eliminate much of the impulse noise. The unsharp masking used a blurred image obtained from 11×11 linear smoothing.

Fig. 1(a) shows a sample coronal image. The result from median filtering that image is shown in Fig. 1(b). The contrast-enhanced result of the unsharp masking on the same underlying image is shown in Fig. 1(c). As shown in these figures, the impulse noises are removed and the loop structures are sharpened by the preprocessing.

The Strous's loop pixel labeling [10], even when applied to an image "cleaned" by median filtering and unsharp masking, still misclassifies many noise pixels and bright pixels that aren't on the coronal loop structures. Coronal loop structures' low contrast and blurriness are largely responsible for these falsely-labeled pixels. However, these falsely-labeled pixels can be largely removed by a combination of global and adaptive thresholdings applied to the "cleaned" image.

We first apply a global thresholding. Its threshold is the median intensity T of the filtered images; all pixels whose intensity is less than T are considered to be non-loop pixels. Next, additional falsely-labeled pixels are removed by an adaptive thresholding step. The adaptive thresholdings is performed in each sub-region of the image. We have found empirically that dividing the image into 31×31 pixel tiles with 50% overlap (e.g., the top-half of a sub-region R_B overlaps the bottom-half of a region R_A that is above sub-region R_B) produces reasonable results. The threshold used in the i^{th} sub-region is the sub-region's median intensity T_i. In fact, wherever sub-regions overlap, the threshold for the overlapped area is the mean of the thresholds of the overlapping sub-regions. Fig. 1(d) shows the result after applying the two thresholdings to a "cleaned" image (i.e., of Fig. 1(c)). Many, but not all, falsely-labeled pixels in this figure have been removed by the thresholdings.

3.2. Oriented Connectivity Method (OCM)

Our Oriented Connectivity Method's constructive curve detection starts from any pixel labeled as a coronal loop pixel and then forms a clustering of all the other pixels that define the same loop structure. This process is applied repeatedly until all pixels labeled as loop pixels have been

processed. Although any scanning process can be used to find the starting points on each loop, we have found that searching for a starting point in a column-wise process followed by a row-wise process is typically sufficient to find the major loop structures. (We've also found it's sufficient to perform the column- (row-) wise search only every twentieth column (row).)

The forming of a clustering of pixels into a loop is a stepwise process which at each step adds one pixel to the current loop. The "best" pixel to be added is found by a search from the current loop's end pixel. A small fan-shaped region (the "searching region") about that pixel is where the search occurs. The searching region's fan shape is bounded by the magnetic field minimum and maximum angular directions (azimuths) for that pixel. The region's extent d was empirically determined to be 5 pixels. An example of the searching region for a pixel S is shown in Fig. 3. In the figure, the arrows represent the azimuths at different heights. The thick arrows represent the extremal azimuths. The "best" pixel in the region is the one that best-preserves loop continuity in position and tangent direction and which is nearby and sufficiently bright. We have encoded the degree of goodness of each candidate pixel using a weighting scheme based on distance, intensity, angular, and tangent weighting factors. The highest weighted pixel is the one joined to the current loop. The constructive process is repeated until no other pixels can be joined to a loop segment end point. The steps of the Oriented Connectivity Method algorithm are as follows:

1. Apply Strous's algorithm (to a "cleaned" image).
2. Start forming a (new) loop from an unassigned pixel P_i that's labeled as a loop pixel.
3. Define the searching region at P_i.
4. Find the unassigned loop-labeled pixels in the searching region of P_i.
5. If there are no loop-labeled pixels in the searching region, find a loop-labeled pixel in the 8-neighborhood of P_i. If one exists, apply Step 7.
6. If there is no loop-labeled pixel in the neighborhood, repeat Step 2. If so, set the loop-labeled neighborhood pixel as a new starting point and repeat Step 3.
7. Apply weighting scheme to find each pixel's goodness.
8. Assign the highest-weighted pixel in the searching region as the next pixel, P_{i+1}, of the loop.
9. Connect P_i and P_{i+1}, save P_{i+1} as new P_i.
10. Repeat Steps 1 to 8 until no other points are selected.
11. Calculate the mean width of the detected loop.
12. Remove the detected loop from the image and save its description.
13. Repeat Steps 2 to 11 until all image pixels have been considered.

In Step 11, mean width is determined from the intensity profiles at three points (the midpoint and points halfway between the midpoint and endpoints) of the detected loop. At each point, loop width is defined to be the distance (measured perpendicularly to the loop's local direction) between the maximum gradient points on each loop side.

3.3. Post-processing

The OCM can miss some loops and over-segment (i.e., disconnect) others. The pixel-by-pixel linking process may also produce aliased (i.e., jaggy) loop structures. To remove the aliasing and join the disconnected sub-segments of the loops, we post-process the OCM's output by applying B-spline fitting and edge linking. The first B-spline fitting is designed to produce smooth loop curves. In our usage of B-spline fitting, a different number of equally-spaced loop points are used for the control points according to the length of each loop to be fit (i.e., more control points are used to represent a longer loop). Then a simple edge linking and the second B-spline fitting are applied to merge disconnected loop segments smoothly: namely, if two loop segments terminate a short distance from each other, they are linked provided that they have similar tangent directions at their end points.

4. Experimental Results

We have evaluated the effectiveness of the OCM using synthetic and real coronal images.

To benchmark the OCM's effectiveness, we applied a manual method (which we will label MM) that involved manually identifying as many coronal loop points as possible and a semi-manual method (which we will label SMM) that involved manually sampling several coronal loop points and using the points sampled on each loop as the control points of a B-spline fitting. These two manual methods and the OCM were applied on size 500×500 synthetic datasets that were created by projecting a collection of 3D field lines generated from three known dipoles onto a 2D image.

The benchmarking considered the global positional error (GPE) and four metrics on this error (e.g., maximum, minimum, mean, and standard deviation). This error measures the distance of traced/detected curves from the known loop centers. The GPE is measured over all loops. Fig. 2(a) shows a synthetic dataset and the overlaid blue curves in Fig. 2(b) represent the loops detected in this image by the OCM. As shown in Fig. 2(b), our technique detected most of the loops that are easily visible to human vision. The GPE measures for the two manual methods and the OCM on the synthetic image shown in Fig. 2 are listed in Table 1. The OCM produced smaller errors and had less

variance in position on its loops. However, the numbers of traced/detected loops were 74, 69, and 57 for the MM, SMM, and OCM, respectively.

We have also applied the OCM to seven real coronal images. To analyze the effectiveness of the OCM, eight coronal loops were selected arbitrarily on each image and then the images were considered by the semi-manual method and by the OCM. Three classes of error were measured: the number of false positives, errors in length, and the positional errors. There were 4 global false positive errors (i.e., 4 loop structures were detected by the semi-manual method but not detected by the OCM) in the collection of tests. The OCM tended to over-segment loops; the average loop lengths from OCM were 44% shorter than the loop lengths from SMM. The average relative global position error for the OCM was 3.30 pixels. The result for the image shown in Fig. 1(a) is shown in Fig. 1(e). The overlaid blue curves in Fig. 1(e) represent the loops detected by the OCM; the technique reasonably detected the well-defined loops.

5. Conclusions

We have presented a new method of detecting solar coronal loop structures. The Oriented Connectivity Method, the first automated coronal loop detection technique, uses physical constraints to guide the coronal curve detection process. Through evaluation of the technique, we have shown that the technique can provide consistent and reasonable automated detections of loop structures in solar coronal images.

For the future work, additional image processing techniques to sharpen the coronal loops and other techniques to more strongly exploit the orientation of the magnetic field will be explored.

Similarly-shaped structures in other scientifically-interesting environments are influenced by other characterizable physical properties, thus extending the OCM to other arenas may be possible.

Acknowledgement

This work was supported by NASA's Office of Space Science – Solar and Heliospheric Physics Supporting Research and Technology program.

References

[1] J. Canning, J. J. Kim, N. Netanyahu, and A. Rosenfeld, "Symbolic Pixel Labeling for Curvilinear Feature Detection," *Pattern Recog. Letters*, Vol. 8 (5), Dec. 1988, pp. 299-310.

[2] H. Freeman, "On the Encoding of Arbitrary Geometric Configurations," *IRE Trans. on Electronic Computers*, Vol. 10, 1961, pp. 260-268.

[3] P.V.C. Hough, "Method and Means for Recognizing Complex Patterns," *U.S. Patent, 3,069,654*, Dec. 1962.

[4] J. Jang and K. Hong, "Detection of Curvilinear structures and Recognition of Their Regions in Gray-scale Images," *Pattern Recog.*, Vol. 35 (4), Apr. 2002, pp. 807-824.

[5] M. Kass, A Within, and D. Terzopoulos, "Snakes: Active Contour Models," in *Proc. of 1st Int'l Conf. on Computer Vision*, London, 1987, pp 259-269.

[6] T. Magara and D.W. Longcope, "3-Dimensional Evolution of a Magnetic Flux Tube Emerging into the Solar Atmosphere," *EOS Trans. American Geophysical Union*, 2002, pp. A441.

[7] V. Makhervaks, G. Barequet, and A. Bruckstein, "Image Flows and One-liner Graphical Image Representation," in *Proc. of the 16th Int'l Conf. on Pattern Recog.*, Quebec City, Aug. 2002, Vol. 1, pp. 640-643.

[8] R. Plonesy and R.E. Collin, *Principles and Application of Electromagnetic Fields*, McGraw Hill, New York, 1961.

[9] W.H. Press, B.P. Flannery, S.A. Teukolsky, and W.T. Vetterling, *Numerical Recipes in C: The Art of Scientific Computing, 2nd Ed*, Cambridge University Press, Cambridge, 1993.

[10] L.H. Strous, "Loop Detection," http://www.lmsal.com/~aschwanden/stereo/2000easton/cdaw.html, accessed on Oct. 12, 2002.

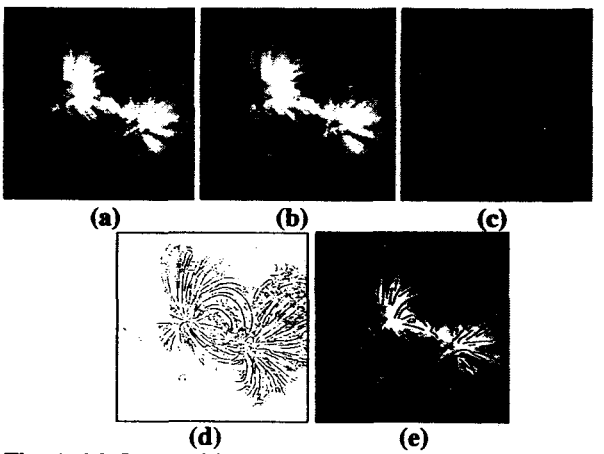

Fig. 1. (a) Coronal image, (b) Median filtered image, (c) (Contrast enhanced) Unsharp masked image, (d) Thresholded curve features, (e) Detected loops.

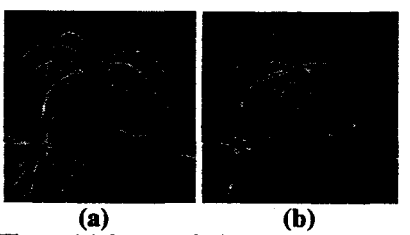

Fig. 2. (a) Synthetic image, (b) Detected loops

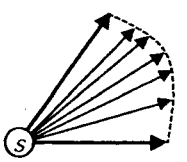

Fig. 3. Search Region about S

Table 1. GPE on synthetic image (in pixels)

Method	Max	Min	Mean	Std Dev
MM	3.61	0.00	0.66	0.63
SMM	3.51	0.00	0.58	0.40
OCM	3.00	0.00	0.57	0.37